Special Issue of the 6th International Congress & Exhibition (APMAS2016), Maslak, Istanbul, Turkey, June 1–3, 2016

Influence of ZrO_2 Addition on the Structure and Dielectric Properties of $BaTiO_3$ Ceramics

K.E. Oksuz[a,*], S. Sen[b] and U. Sen[b]

[a]Cumhuriyet University, Department of Metallurgical and Materials Engineering, 58140, Sivas, Turkey
[b]Sakarya University, Department of Metallurgical and Materials Engineering, 54187, Sakarya, Turkey

$Ba(Ti_{1-x}Zr_x)O_3$ ($x = 0 \div 0.3$) ceramics were prepared by the standard solid state reaction method and were sintered at 1450 °C for 4 h. The structural and dielectric properties of the samples were studied. The phases formed in the ZrO_2 doped $BaTiO_3$ were tetragonal and of cubic symmetry. Increase in ZrO_2 content in the $BaTiO_3$ caused to increase of the lattice parameter and crystallite size of the perovskite structure. The evolution of the Raman spectra was studied for various compositions and the spectroscopic signature of the corresponding phase was determined. The scanning electron microscope was used to investigate the microstructure and surface morphology of the sintered samples. Scanning electron microscope observations revealed enhanced microstructural uniformity and retarded grain growth with increase of ZrO_2 content. Dielectric characteristics of ZrO_2 doped barium titanate were studied using a Hioki 3532-50 LCR meter in the frequency range of 1 kHz–1 MHz. It is found that the dielectric constant (ε_r) increases while the dielectric loss ($\tan\delta$) decreases with increase in zirconium oxide content ($x < 0.3$).

DOI: 10.12693/APhysPolA.131.197
PACS/topics: 85.50.–n, 77.84.–s, 82.45.Xy, 81.30.–t

1. Introduction

$BaTiO_3$ (BT) is the most promising lead-free material exhibiting superior properties like high dielectric permittivity, low dielectric loss tangent, dielectric reliability, high electromechanical coupling coefficients, good thermal shock resistance and large tunability [1]. Hence, this material finds its applications in tunable microwave devices and thermistor applications [2, 3]. A lot of work was carried out in evaluating the properties of the doped $BaTiO_3$ ceramics. The effect of dopants ranging from metals, semiconductors to insulators including rare-earth dopants like La, Nd, Pr, Gd on the dielectric and ferroelectric properties were investigated [4–6]. Zr is chosen as a B site dopant for such ABO_3 type perovskites due to its effective role in minimising the dielectric loss at low frequencies. Since zirconium is known as an effective substituent in $BaTiO_3$ to shift the Curie temperature downward and raise the other two phase transition temperatures, many investigations have focused on the effect of Zr^{4+} ion additions [7–9]. In this work $Ba(Ti_{1-x}Zr_x)O_3$ ceramics were prepared by a solid-state reaction technique. The Raman spectroscopy, X-ray and microstructural analyses, and dielectric properties were performed to study the effect of ZrO_2 substitution on the $Ba(Ti_{1-x}Zr_x)O_3$ ($x = 0 \div 0.3$) ceramic.

2. Materials and methods

$Ba(Ti_{1-x}Zr_x)O_3$ ($x = 0 \div 0.3$) ceramic powders were prepared by solid-state mixed oxide technique. The starting materials used were $BaCO_3$, TiO_2, and ZrO_2 (all $> 99.9\%$ pure, Aldrich, USA). The stoichiometrically weighed amounts of these powders were milled by ball milling technique in isopropyl alcohol using ZrO_2 balls at 200 cycles/min for 24 h and then dried in a Pyrex pan. The powders were followed by calcination in the air for 2 h at 1000 °C. The final powder was attrition milled for 10 h and then sieved to less than 45 µm prior to being mixed with an organic binder (5% PVA 72000 g/mol). Pellets were pressed uniaxially at 100 MPa and sintered at 1450 °C for 4 h in static air in a closed alumina crucible and cooled to room temperature (at a ramp of 5 °C/min). The crystal structure of the samples was determined from X-ray diffraction (XRD) data. An X-ray diffractometer (Rigaku D/MAX/2200/PC) with a monochromatic Cu K_α radiation ($\lambda = 1.5408$ Å) was used over a 2θ angle from 20° to 80° to characterize the crystal structure of the sintered compacts. A Kaiser RAMAN-RXN1 Raman spectrometer was used for further investigation of phase composition of the samples. The Raman scattering spectra of the ZrO_2 doped $BaTiO_3$ ceramics were recorded using 785 nm Invictus laser light source, a low excitation power of 5 mW. The surface morphology of the ceramics was examined by using a scanning electron microscope (SEM, Model JEOL-JSM 6060-LV, Japan). The frequency dependence of dielectric properties was characterized using a precision LCR Meter (Hioki 3532-50 LCR, Japan) at 1 kHz–1 MHz at room temperature.

3. Results and discussion

3.1. XRD analysis

Phases formed in the sintered $Ba(Ti_{1-x}Zr_x)O_3$ ($x = 0 \div 0.3$) ceramics were confirmed by XRD analysis as shown in Fig. 1. The XRD analysis showed that there

*corresponding author; e-mail: kerimemreoksuz@gmail.com

is no any trace phase beside the perovskite phases. Increase of ZrO_2 content in the $Ba(Ti_{1-x}Zr_x)O_3$ ceramics caused to increase the peak intensities of the related perovskite phases. The peaks taking place on the XRD pattern of $Ba(Ti_{1-x}Zr_x)O_3$ ($x = 0.1$) ceramic changed the position according to XRD patterns of the $BaTiO_3$ ceramic, ZrO_2 free (see Fig. 1a and b). The change of the peak intensities and positions resulting from the ionic radius of Zr^{4+} (0.72 Å) is large as compared to Ti^{4+} (0.60 Å) and so, caused by variation of lattice parameters of the perovskite phases. In addition to these, the increase of ZrO_2 content caused more variations of lattice parameters of the $Ba(Ti_{1-x}Zr_x)O_3$ ($x = 0 \div 0.3$) ceramics. The analysis shows that an increase in ZrO_2 content decreases the c-parameter and increases the a-parameter, causing a change from tetragonal (Fig. 1a) to cubic (Fig. 1b–d) symmetry, which supports the earlier reports on BZT [10, 11].

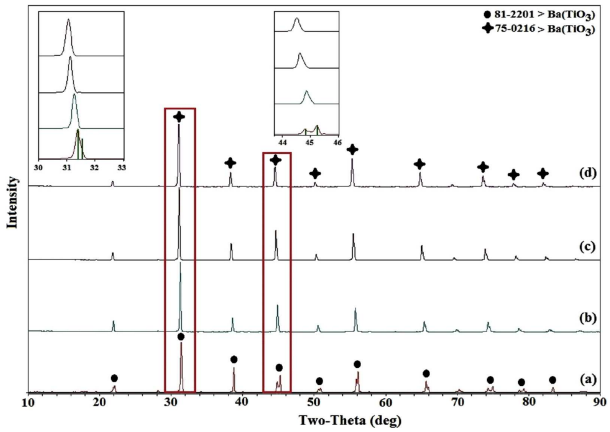

Fig. 1. XRD patterns of $BaZr_xTi_{1-x}O_3$ ($x = 0 \div 0.3$) sintered ceramics samples at RT: (a) $x = 0$, (b) $x = 0.1$, (c) $x = 0.2$, (d) $x = 0.3$ (inset: the magnified patterns in the vicinity of 31.5° and 45°).

3.2. Raman spectroscopy

$BaTiO_3$ is a well-known classic ferroelectric material that is cubic above 39–408 K and belongs to the space group $Pm3m$ [1]. At temperatures below 393 K it is ferroelectric with a $P4mm$ (C^1_{4v}) structure, which further transforms into orthorhombic and rhombohedral structures at 278 and 183 K, respectively. The cubic (paraelectric) phase allows 12 optical modes ($3F_{1u}+1F_{2u}$) that are not Raman active [12]. In the tetragonal (ferroelectric) phase, three $A_1 + E$ phonons arise from the three F_{1u} modes, whereas one $E + B_1$ mode comes from the F_{2u} mode, the so-called "silent mode" since it is neither infrared nor Raman active. These modes further split into longitudinal (LO) and transverse (TO) components due to the long range electrostatic forces associated with lattice iconicity [13]. Room temperature measured Raman spectra of $Ba(Ti_{1-x}Zr_x)O_3$ ($x = 0 \div 0.3$) ceramics are displayed in Fig. 2. Observed spectral features are numbered consecutively from 152 to 752, starting from the low wave number region. Peaks 302, 512, and 712 cm^{-1} are found in all ferroelectric phases of BT-based materials. Peaks 280 cm^{-1} and 512 cm^{-1} have a dominant A_1(TO) character, as was proven in polycrystalline BT by polarization measurements [14, 15], and the former is associated with polar Ti–O vibrations.

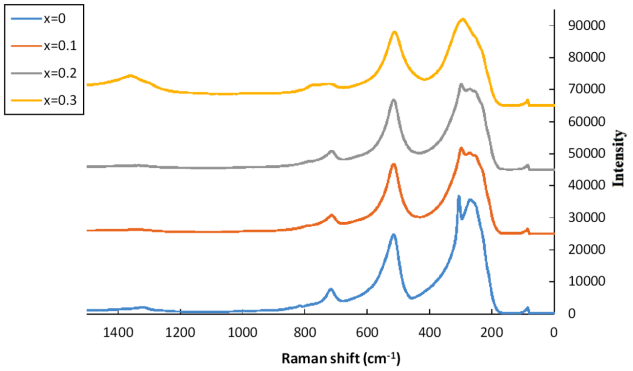

Fig. 2. Raman spectra of $Ba(Ti_{1-x}Zr_x)O_3$ ($x = 0 \div 0.3$) dielectric ceramics sintered at 1450 °C for 4 h.

3.3. Microstructural characteristics

All the samples sintered at 1450 °C for 4 h were studied by scanning electron microscope. SEM study of the samples revealed that the sintering took place without grain growth. The SEM micrographs of $Ba(Ti_{1-x}Zr_x)O_3$ ($x = 0 \div 0.3$) dielectric ceramics are shown in Fig. 3a,d, respectively. There is no obvious grain structure in all samples. As shown in Fig. 3b–d, after adding 0.1 to 0.3 mol.% ZrO_2 into BT, the grain structure starts to develop and the grain size is about 1.2–1.55 μm.

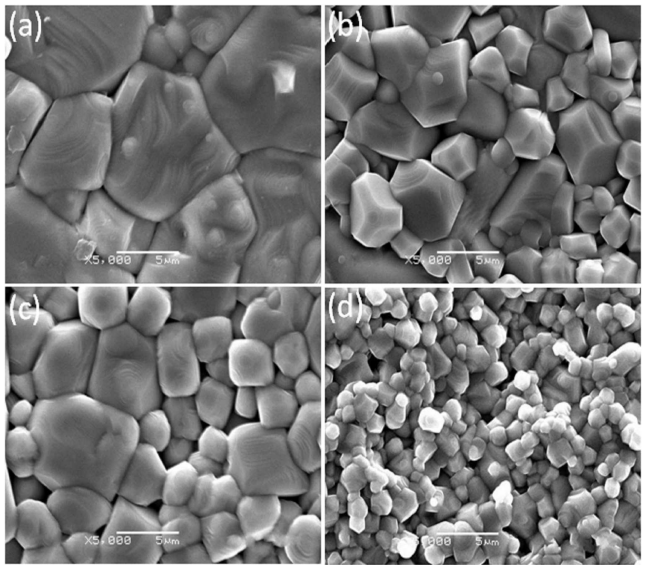

Fig. 3. SEM micrographs for $Ba(Ti_{1-x}Zr_x)O_3$ ceramics sintered at 1450 °C for 4 h: (a) $x = 0$, (b) $x = 0.1$, (c) $x = 0.2$, (d) $x = 0.3$.

Compared to pure $BaTiO_3$ and $Ba(Ti_{0.7}Zr_{0.3})O_3$ ceramics, $Ba(Ti_{0.7}Zr_{0.3})O_3$contained more porosity than $BaTiO_3$. This corresponds to the result shown in Fig. 3a that pure $BaTiO_3$ has a higher density than $Ba(Ti_{0.7}Zr_{0.3})O_3$. By adding ZrO_2 into $BaTiO_3$, the core-shell structure developed and does not exhibit exaggerated grain growth. It can be shown from the SEM images that the ZrO_2 modified BZT ceramics exhibit fine grain size and tetragonal structure to cubic structural transformation [16–19].

3.4. Dielectric study

Figure 4a and b shows the frequency dependence of the dielectric constant and $\tan\delta$ of $Ba(Ti_{1-x}Zr_x)O_3$ ceramics ($x = 0 \div 0.3$) measured at 1 kHz to 1 MHz. It can be seen that the value of dielectric constant is higher at lower frequency and with an increase in frequency, it decreases because in a dielectric material, polarization occurs due to contributions of electronic, ionic, dipolar, and space charge region. At lower frequencies, all the types of polarization contribute to polarization and as the frequency increases, contribution of different polarization decreases and at higher frequency only dipolar and electronic polarizations mainly contribute to polarization [11]. In this study, the results show that the $Ba(Ti_{1-x}Zr_x)O_3$ ($x = 0.2$) ceramics has the excellent dielectric properties. When the Zr^{4+} ion content approaches $x = 0.2$, the dielectric constants are increased to a maximum while the dielectric loss reaches the minimum value (Fig. 4a and b) [20]. The result indicates that the peak value of the dielectric constant for low doped sample is the maximum and the peak value decreases with ZrO_2 content ($x > 0.2$).

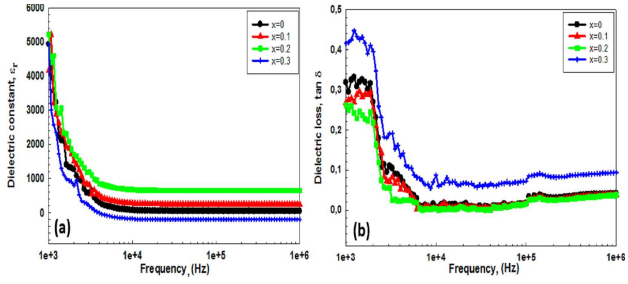

Fig. 4. Frequency dependence of (a) dielectric constant, (b) dielectric loss of $Ba(Ti_{1-x}Zr_x)O_3$ ceramics ($x = 0 \div 0.3$).

4. Conclusions

Perovskite types $Ba(Ti_{1-x}Zr_x)O_3$ ($x = 0 \div 0.3$) ceramics were obtained by sintering at 1450 °C/4 h from ceramic powders by the solid state reaction route. X-ray diffraction data and the Raman spectroscopy showed the formation of single phase solid solutions and pointed out the increase of the lattice parameters, as well as the change of the unit cell symmetry as the ZrO_2 content increased from $x = 0.1$ to $x = 0.3$. Addition of different concentration of ZrO_2 has influence on the microstructure of barium titanate ceramics. When the ZrO_2 concentration was increased, a significant decrease in grain size was observed. The dielectrical properties of the different samples had been elucidated by LCR meter as a function of frequency. The measurement from the different samples showed that there was a significant change in the dielectric constant and dielectric loss with some increase of the ZrO_2 content. When the concentration of Zr^{4+} ions was increased ($x < 0.3$), the dielectric constant also slightly increased due to the phase transformation and grain size. A linear decrease of dielectric constant and dielectric loss with frequency up to 1 MHz has been noticed in all specimens.

References

[1] B. Jaffe, W.R. Cook Jr, H. Jaffe, *Piezoelectric Ceramics*, Academic Press, London 1971, p. 317.

[2] M.A. Zubair, C. Leach, *J. Appl. Phys.* **104**, 103711 (2008).

[3] Y. He, X. Yebin, T. Liu, C. Zeng, W. Chen, *J. Alloys Comp.* **509**, 904 (2011).

[4] X. Diez-Betriu, J.E. Garcia, C. Ostos, A.U. Boya, D.A. Ochoa, L. Mestres, R. Perez, *Mater. Chem. Phys.* **125**, 493 (2011).

[5] A. Lanculescu, Z.V. Mocanu, L.P. Curecheriu, L. Mitoseriu, L. Padurariu, R. Trusca, *J. Alloys Comp.* **509**, 10040 (2011).

[6] H. Chen, C. Yang, F. Chunlin, J. Shi, J. Zhang, W. Leng, *J. Mater. Sci. Mater. Electron.* **19**, 379 (2008).

[7] Z. Jiwei, Y. Xi, Z. Liangying, S. Bo, H. Chen, *J. Cryst. Growth* **262**, 34 (2004).

[8] W.S. Choi, B.S. Jan, D.G. Lim, J. Yi, B. Hong, *J. Cryst. Growth* **237-239**, 438 (2002).

[9] F. Zimmermann, M. Voigts, W. Menesklou, E.L. Tiffee, *J. Eur. Ceram. Soc.* **24**, 1729 (2004).

[10] Z. Yu, R. Guo, A.S. Bhalla, *J. Appl. Phys.* **88**, 410 (2008).

[11] S. Mahajan, O.P. Thakur, C. Prakash, K. Sreenivas, *Bull. Mater. Sci.* **34**, 1483 (2011).

[12] R. Louden, *Adv. Phys.* **13**, 423 (1964).

[13] M.D. Domenico Jr., S.H. Wemple, S.P.S. Porto, R.P. Buman, *Phys. Rev.* **174**, 522 (1968).

[14] L.H. Robins, D.L. Kaiser, L.D. Rotter, P.K. Schenck, G.T. Stauf, D. Rytz, *J. Appl. Phys.* **76**, 7487 (1994).

[15] T. Sakashita, M. Deluca, S. Yamamoto, H. Chazono, G. Pezzotti, *J. Appl. Phys.* **101**, 123517 (2007).

[16] K.E. Öksüz, Ş. Şen, U. Şen, *J. Aust. Ceram. Soc.* **51**, 137 (2015).

[17] K.E. Öksüz, Ş. Şen, U. Şen, *Acta Phys. Pol. A* **127**, 1086 (2015).

[18] H. Wang, J. Wu, *J. Alloys Comp.* **615**, 969 (2014).

[19] H.T. Martirena, J.C. Burfoot, *Ferroelectrics* **7**, 151 (1974).

[20] M. Deluca, C.A. Vasilescu, A.C. Ianculescu, D.C. Berger, C.E. Ciomaga, L.P. Curecheriu, L. Stoleriu, A. Gajovic, L. Mitoseriu, C. Galassi, *J. Eur. Ceram. Soc.* **32**, 355 (2012).